CAAP Quarterly Report

Date of Report: *April 9, 2015*

Contract Number: *DTPH5614HCAP04*

Prepared for: *Dr. James Merritt, PHMSA-DOT*

Project Title: *Optimized Diagnosis and Prognosis for Impingement Failure of PA and PE Piping Materials*

Prepared by: *University of Colorado-Denver, Arizona State University*

Contact Information: *Dr. Yiming Deng and Dr. Yongming Liu*

For quarterly period ending: *April 9, 2015*

Business and Activity Section

(a) Generated Commitments

Pipeline infrastructure and its safety are critical for the recovering of U.S. economy and our standard of living. Statistics from U.S. Department of Transportation (DOT) and Gas Technology Institute (GTI) show the decline in use of steel and cast iron piping materials is significant in recent years and the increase in pipeline system size is largely due to plastic pipe installations. However, failure inevitably occurs in plastic piping materials and impingement failure is caused by high localized stress concentration combined with defects and inclusions. Previous research efforts were mainly focusing on PE materials, efficient and effective impingement damage diagnosis and prognosis of various types of new plastic piping materials still remain unaddressed and challenging. The proposed research will fundamentally understand and characterize the failure modes and associated material behaviors for modern plastic piping materials. The proposed optimized diagnosis and prognosis approaches will thoroughly investigate and compare the dominating PE materials (make up nearly 97% of current plastic pipes) and the emerging PA pipes that can operate at much higher pressures and be installed using existing PE tools and techniques. If successful, this study can help to effectively maintain and improve the reliability of pipeline systems, and ultimately reduce the environmental consequences because of a pipeline catastrophic failure.

The overall objectives of the proposed research are two-fold: optimized diagnosis-find existing impingement damage at the earliest stage before it becomes failure critical in PE and PA materials, conduct comprehensive comparison studies to identify the differences in micro-cracking mechanism between these two materials; and optimized prognosis - accurately predict the remaining strength and RUL of PE and PA components through mechanical modeling and experimental investigations.

The eighteen-month effort will establish a framework composed of both physical (CU) and mechanical modeling (ASU) with optimized parametric studies both numerically and experimentally, and models validation during the first project year (month 1 to month 12). A thorough anomaly detection, characterization and sensitivity analysis for both optimized diagnosis and prognosis algorithms will be carried out in the second project year (month 13 to month 16). Building upon achieving these research milestones, a model-assisted detection and prediction framework with the integrated diagnosis and prognosis capabilities will be realized and tested in field at the last phase of this project (month 16 to month 18). The specific technical objectives are addressed through the following two major research tasks, each has three subtasks:

Task 1 focuses on the sensing physics modeling of impingement failure diagnosis and experimental investigation assisted by model-based inversion techniques. Three subtasks are proposed:

(1.1) element-free Galerkin’s method (EFG) development for the electromagnetic modeling of arbitrary and micro-scale crack initiation and propagation due to impingement; (1.2) model-based inversion for ultra-fast impingement failure reconstruction and sensing assisted by compressed sensing techniques; (1.3) demonstration of optimized diagnosis capabilities using electromagnetic diffraction tomography array.

Task 2 focuses on the mechanical modeling of impingement failure and experimental investigation. Three subtasks are proposed: (2.1) extended finite element method (XFEM) and cohesive zone modeling (CZM) for the crack initiation and propagation simulation; (2.2) experimental investigation of impingement effect on the failure of investigated materials; (2.3) parametric study and sensitivity analysis for the optimized prognosis algorithms.

(b) Status Update of Past Quarter Activities

Task 1a - Comparison of PE and PA pipe materials

Polyethylene (PE) is a cost effective solution for a broad range of piping problem in a variety of industries. It has been tested and proven effective for above ground, surface, buried applications. High-density polyethylene pipe (HDPE) can carry portable water, wastewater, chemicals, and compressed gases. Polyethylene is strong, extremely tough and very durable. Since it is a plastic material, polyethylene does not rust, rot or corrode, this will lower the life cycle costs (LCC).

PA-11 is a material of choice for corrosion free, aggressive hydrocarbon transport system. PA-11 thermoplastic material has been used across the entire oil and gas value chain extensively, for cost-effective non-metallic piping systems. PA-11 provides a better value compare to steel pipe. It has lower total installation cost, lower lifetime maintenance, and comparable performance. According to a brochure from Arkema, PA-11 also shows excellent resistance to slow crack growth. In the past month, CU-Denver and ASU have received the PA samples from Arkema and will start experimental comparison of both PE and PA materials. Simulation studies will continue in the forthcoming Q3.

Task 1b- Multichannel scanning sensor model development for PE and PA materials

In quarter 1, we introduced a preliminary model for a multichannel scanning sensor. The sensor was design as pipe shaped tube with scanning probes mounted outside. The goal is to move the sensor along within the pipe to collect data from the inside of the pipe.

During the second quarter, we redesign the scanning sensor system. In quarter 1, we used a pipe shaped tube as scanning sensor, the tube served as ground plane for each scanning probe. But since it is a cylinder, the ground plane is not perfectly perpendicular to the probes, which may cause reflection from the ground plane. So we design a cubic shaped scanning sensor first to verify the reflection and coupling in the system. Fig. 1 shows the geometry of the cubic sensor. The size of the cubic is 10cm x 10cm x 10cm, which is smaller than the diameter of the pipe (15cm). The radiating frequency of the scanning probe is at 3GHz, the length of the probe is 2.5cm. The scanning probes are located at the center of each sides of the cubic. This design would make sure the each probe is perpendicular to the ground plane and will maximize the power radiating from the probes.

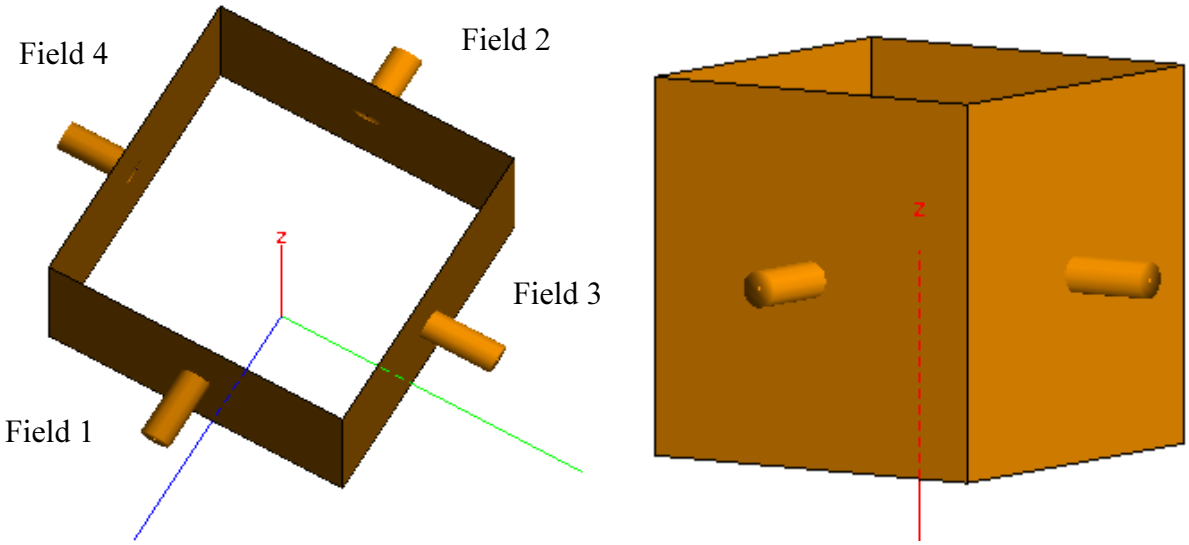

Fig. 1 Geometry of a cubic multi channel scanning sensor

To verify the design, we need to look at the following parameters: reflection coefficient, VSWR, electric field. Reflection coefficient will give us an idea about how well the antenna works for the system, same as VSWR. Electric field will show us if the field around each antenna is symmetric or not.

According to the simulation result, the reflection coefficient of each probe is only 6%, which means most of the power is transmitted to the air and there is barely any reflection in the system. Same as VSWR, the value of VSWR for each antenna is close to 2. Next we are going to look at the electric field value to verify if the probes are radiating equally. Fig.2 shows the electric field plot for each probe.

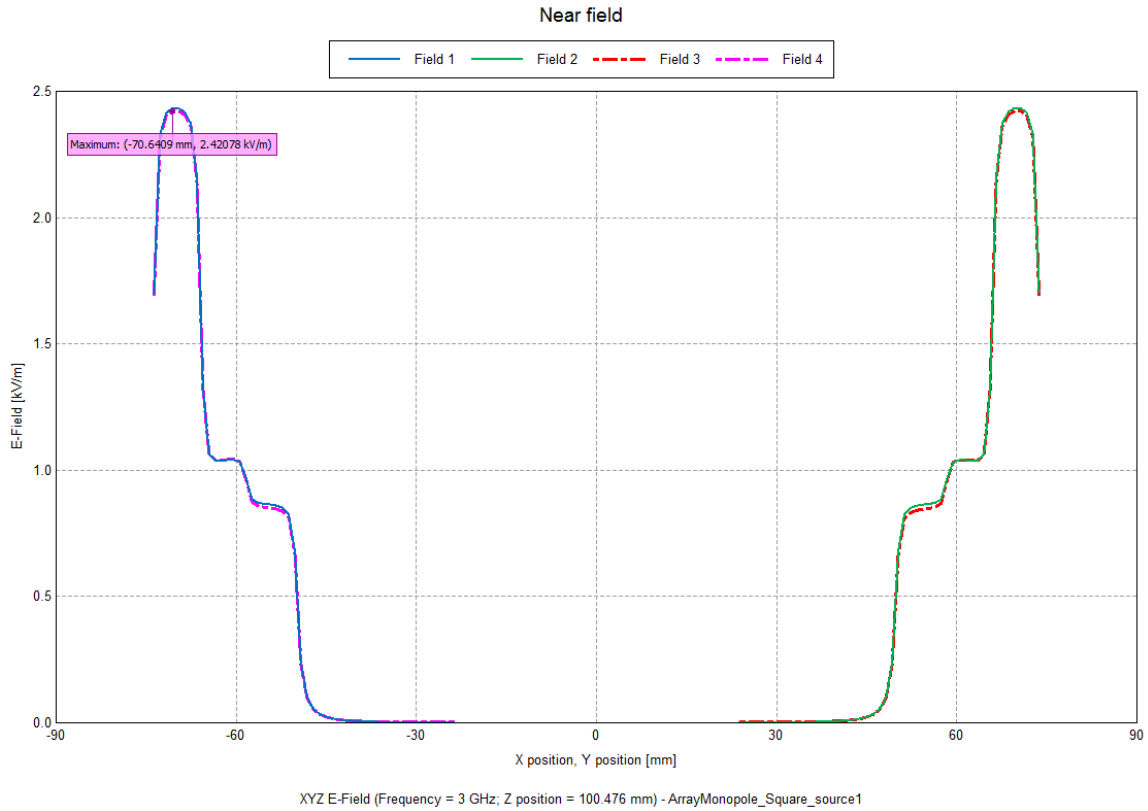

Fig. 2 Electric field of each scanning probe along probe direction

The electric field in Fig. 2 shows that the electric field along probe direction is symmetric and radiating equally in the air. This gave us a promising result for future development.

Next we add a PE pipe material on the outside of the scanning sensor. The geometry showed in Fig. 3. The diameter of the pipe is 15cm, the pipe will be a couple millimeters away from the scanning probe tip. The permittivity of PE material is 2.26, loss tangent is 0.00031. The goal for this simulation is to verify if the reflection coefficient increases compare to the previous simulation. Since we feed each probe using the same voltage source, both reflection coefficient and VSWR should show a similar value among all of the probes. Our goal is to have as high as possible reflection coefficient and VSWR, so we can measure the reflection signal from the target. According to the simulation result, the reflection coefficient has been increased to 14.25%, which means there are more signal has been reflected back from the target compare to the air.

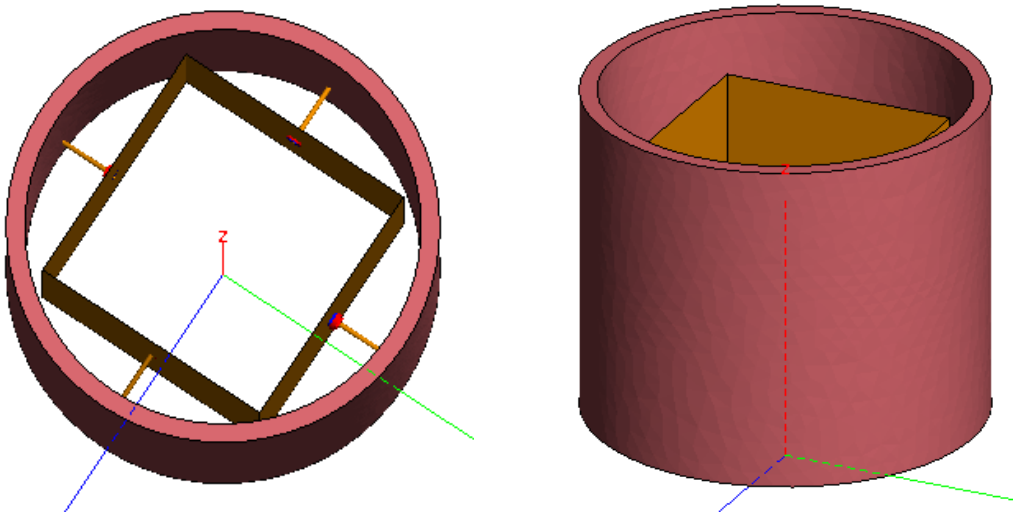

Fig. 3 Geometry of a cubic multi channel scanning sensor with pipe

We also compared the electric field of each probe along the probe direction shown in Fig. 4. From Fig. 4 we can see that the field still symmetric and radiating equally, which same as the simulation in the air. The only difference we have is the maximum value of the electric field. Fig. 4 shows how much field radiated from each probe. Due to the reflection from the target, the field around the probe is lower than the one without the target.

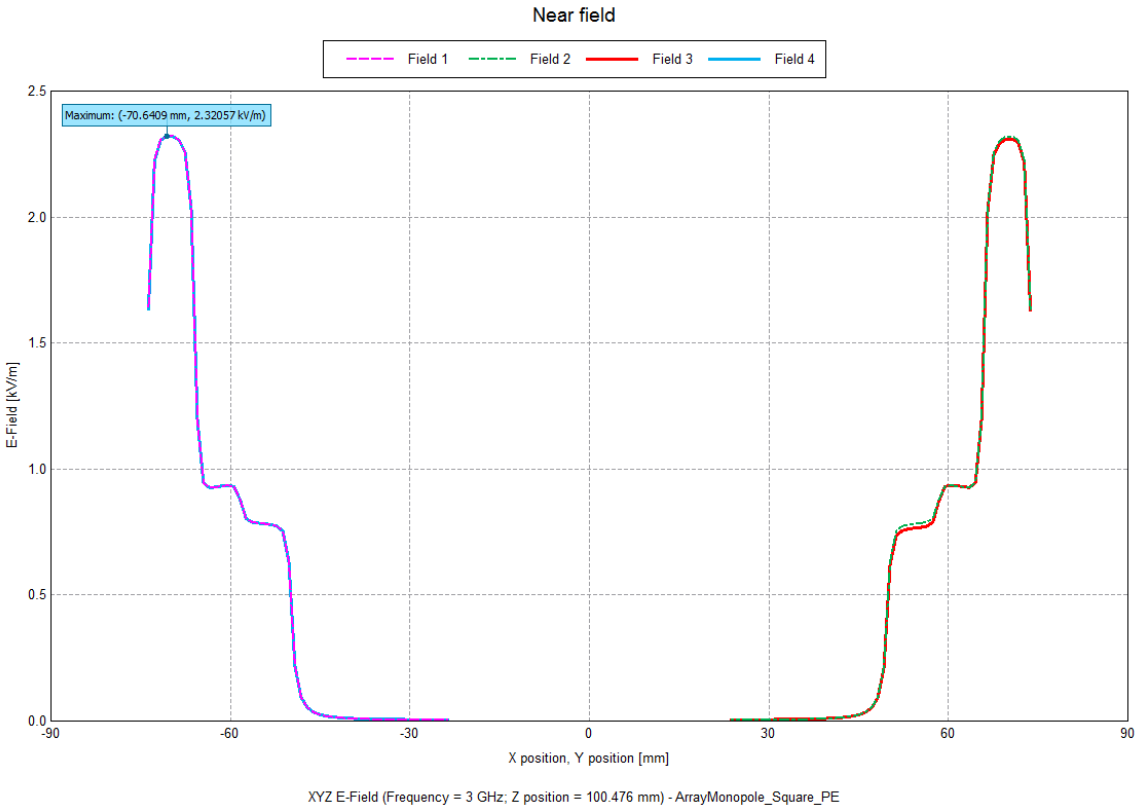

Fig. 4 Electric field of each scanning probe along probe direction with target

Task 2-Mechanical modeling on impingement failure

Task 2 focuses on the mechanical modeling and comparison of PA and PE materials. Two major subtasks are performed: 1) convergence study and parametric study of the developed XFEM failure and fracture simulation methodology; 2) preliminary development of a coupled diffusion fracture simulation framework to consider the effect of hydrogen diffusion on the mechanical performance of PE and PA materials.

Subtask 2.1 Convergence and parametric study of XFEM simulation framework

The developed XFEM simulation framework has been reported in the last progress report. The current research focuses on the convergence study of the XFEM framework and comparative study of PA and PE materials. Convergence study using finite element code in ABAQUS is performed. The element size was varied from 12 units without changing loading and boundary conditions. The crack initiation pressure (Ci) is compared for the convergence study. Summary of this preliminary convergence results are shown in Table 1.

UNITS	Ci, Mpa	% Change
5	4.5324	0
8	4.5324	1.308655
12	4.5925	1.420997
14	4.6587	3.246106
15	4.815	

- Table 1: Converged values of crack initiation pressure

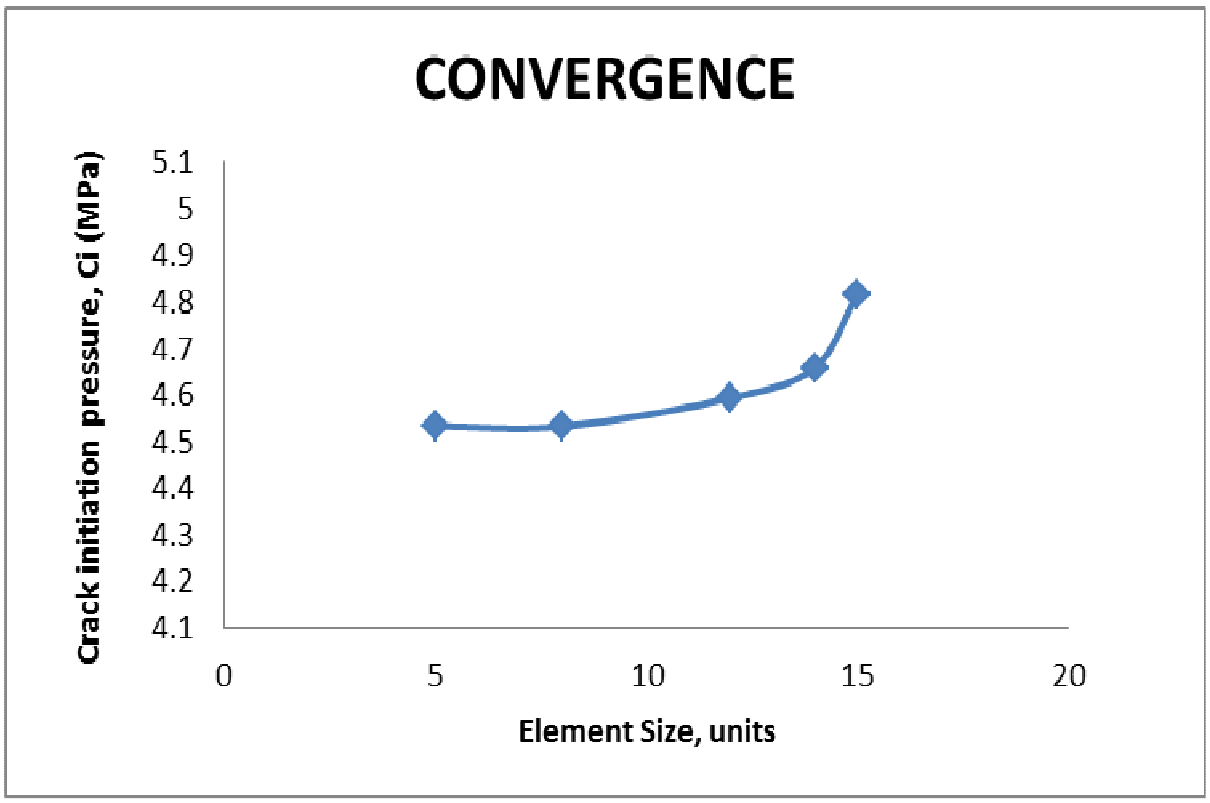

• Figure 15: Convergence studies

The results are shown graphically in Fig. 5. It is seen that the difference of the crack initiation pressure does not change much for most of the invested mesh density (with maximum difference is less than 5%). As the mesh get denser, the difference decreases and approaches a constant value. Convergence for the crack initiation pressure is observed in the current study for the very fine mesh (e.g., below 14 mm for the element size). Detailed study for other types of damage mechanisms and final failure simulation will be investigated in the future.

Natural gas transmission and distribution industry is using pipes of different origins to transport hydrocarbons under pressure. The use of polymeric material such as polyethylene (PE) made it possible to achieve significant profits in construction times and installation costs. However, some catastrophic failures took place for various reasons. It is clear that at least two mechanisms control PE pipe failures based on results available. They are nominally ductile and brittle mechanisms respectively characterizing short and long-term failures.[1]

It remains difficult to assess the relation between creep and fatigue loadings on the one side. On the other side, the manufacturing process of the test specimens (extruded pipes and compression molded sheets) influences considerably the obtained performance for viscoelastic materials subjected to working conditions.[1] Under uniaxial tension, high-density polyethylene (HDPE) often fractures in a ductile manner. The fracture involves extensive necking that is known to occur in the plane-stress condition[2]. However, for large-scale HDPE products like polyethylene pipe, crack can grow rapidly in a brittle manner. This type of fracture is known to be in the plane-strain condition, which has much lower toughness than that in the plane-stress condition.[3] Slow crack growth (SCG) is additional critical issue because PE pipe materials exhibit stress-lifetime curves that have at least two separate rates corresponding to both ductile and brittle fracture mechanisms.[4, 5] The long-term behavior associated with brittle-like failure is most feared as it takes place without any presaging signs. At the same time, the long-term strength is substantially reduced, and so linear predictions from short-term behavior are no longer applicable.[1] The assessment of PE pipe failure mechanisms is to contribute to a better understanding of effects of loading conditions and boundary conditions.

In the current investigation. Comparison between PA-11 and PE materials are performed using the developed numerical simulation framework. The main difference of the two types of materials are their fracture energy. The fracture energy for PE material that has been taken in to consideration ranges

from 30 – 35 KJ/m^2.[3] To carry out the simulation, value of 32.5 KJ/m^2 as fracture energy was selected. The fracture energy for PA-11 was selected as 620 KJ/m^2 . The following graph shows how results varied after updating the fracture energy.

Material	Fracture energy	Pi	Pc
	KJ/m2	MPa	MPa
PA-11	620	4.5816	5.964
PE	32.5	2.9016	3.3312

• Table 2: Fracture energy

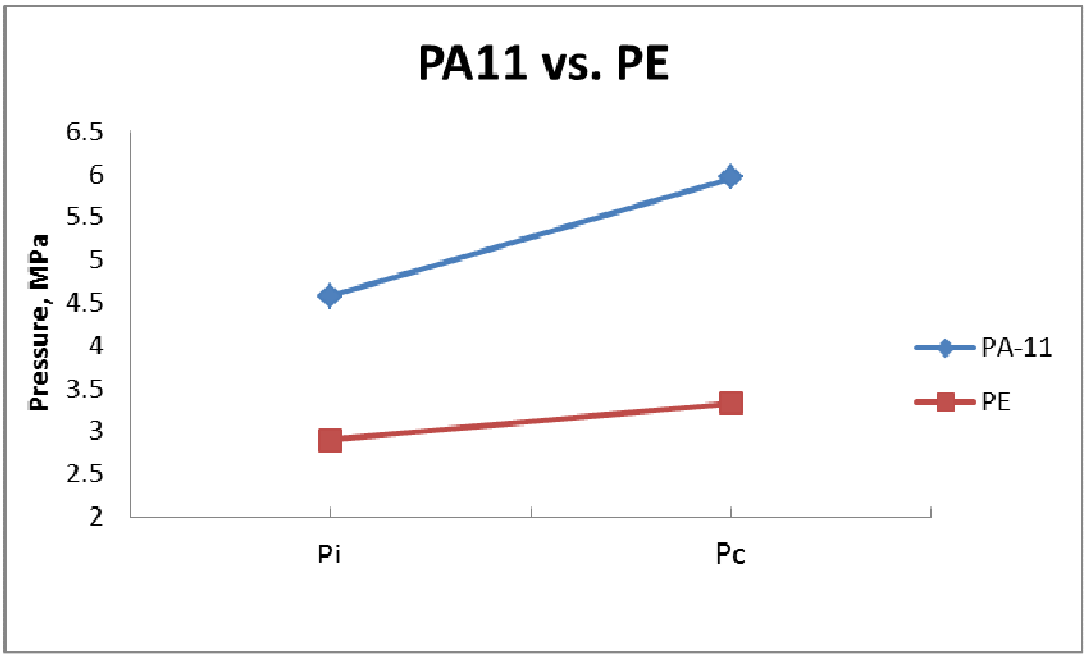

• Figure 6: Comparison between different materials based on fracture energy

Subtasks 2.2 Coupled hydrogen diffusion and failure analysis

The research objectives of this subtask are:

- Evaluate the mass diffusion using numerical simulation on the PE and PA11 pipeline sections and compare the variations in the amount of gas diffused
- Obtain an insight into the degradation of the physical properties of the materials of pipeline and their influence on the life of materials
- Address the reduction in cohesive energy due to mass diffusion and is influence in overall numerical simulation of the pipeline

In this section of report, a simulation of the mass diffusion of methane gas has been simulated of particular conditions. The simulations give us a clear picture on the variation of the gas concentration along the radial direction of the pipeline.
The gas transport coefficients in polymers are generally complex to determine and to analyze, especially in the field of high pressures and high temperatures.

1.0 MASS DIFFUSION IN PIPELINES

The mass diffusion of various gases like hydrogen, methane and carbon dioxide have been a great concern for the increasing deterioration of the life of the polymer pipelines used. The sorption of gasses in polymer membranes depends strongly on the nature of the polymer, the pressure and temperature. At moderate temperatures and pressures (below the critical values) only small amounts of gas is assumed

to be dissolved in the polymer. Once the gas is dissolved on the high pressure side of the membrane it diffuses towards the low pressure side because of the difference in chemical potential. The amount of gas transported by diffusion is controlled by the applied pressure and temperature, and the nature of the gas and the polymer.

2.0 SOLUBILITY AND DIFFUSION FROM EXPERIMENTAL DATA

The principle for the solubility measurements is that a polymer sample of known geometry is placed on a balance in a closed vessel. Gas is applied at a given temperature and pressure and the weight increase due to absorption of gas is measured as a function of time. The concentration of absorbed gas is determined as the mass of gas, m (t), divided by the mass of the polymer sample at atmospheric pressure. The maximum concentration of gas that can be dissolved in the polymer is easily determined as the plateau of a plot of concentration vs time (illustrated in figure 1). If Henry's law applies a plot of C_{max}, versus P gives a straight line with the slope S (the solubility coefficient). Where C is the concentration of dissolved gas per volume unit polymer, S is the solubility coefficient or the inverse Henry's law coefficient (volume gas per volume unit polymer and pressure unit) and P is the pressure of the gas.

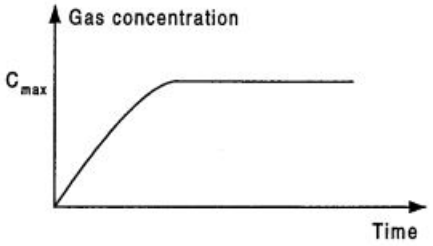

Figure 7: Maximum concentration of the gas

3 TIME LAG METHOD FOR MEASUREMENT OF SOLUBILITY, DIFFUSIVITY OF GASES IN POLYETHYLENE AND POLYAMIDE 11

The principle for the experimental setup is illustrated in figure 8. A high pressure, Po is applied to the membrane forcing the molecules-to diffuse through the membrane to the low pressure, PL, side. The amount of gas permeated through the membrane is measured as a function of time and plotted. Figure 3 illustrates a typical plot of the flux versus time.

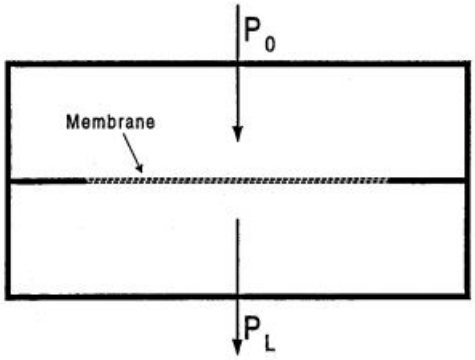

Figure 8: Experimental setup of time lag method for gas diffusion

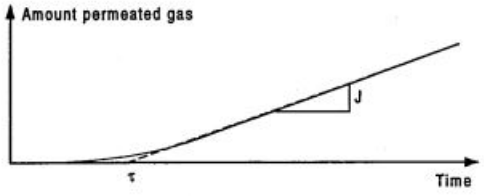

Figure 9: Time lag curve for property of gas diffusion

The concentration profile in the membrane is given by an analytical solution to Fick's second law, assuming that the concentration on the low pressure side is zero and the diffusion coefficient is a constant

$$\frac{\partial c}{\partial t} = D\frac{\partial^2 c}{\partial y^2} \tag{1}$$

The determination of the transport coefficients of various gases is made by a manometric method (pressure accumulation in a closed volume). The precise description of the "medium pressure" equipment used and its working procedure are detailed in [3]. Permeability, diffusion and solubility are obtained from the experimental curves, by using the "time lag" method. In the studied ranges of pressure and temperature, the diffusion coefficient is assumed to be independent of the gas concentration in the polymer, and it is admitted that the solubility respects Henry's law. These restrictive assumptions allow to obtain apparent values of D and S that are quite realistic when there are few interactions between the gas and the polymer. Then, the permeability coefficient, Pe, expressed in cm^3 (STP)/cm·s·MPa, is directly proportional to the slope of the straight line representing the gas flow rate versus the applied pressure, in steady state, and is written as:

$$Pe = \frac{Ql}{At\,p} \tag{2}$$

where Q is the amount of gas in cm^3 (STP), l is the membrane thickness in cm, A is the diffusion area in cm, t is the time in s, and p is the applied pressure in MPa. The diffusion area was equal to 12.57 cm^2 [2, 3]. The diffusion coefficient, D, given in cm^2/s, is obtained from the relation:

$$D = \frac{l^2}{6\theta} \tag{3}$$

θ , the "time lag" in s, corresponds to the intercept of the x axis with the straight line in steady state. The solubility coefficient S, expressed in cm^3 (STP)/cm^3·MPa, is easily calculated as the ratio Pe/D.

Table 3. Typical material parameters for PA and PE materials

Material	Temperature (°C)	Pressure (MPa)	Diffusion coefficient (D) (cm^2/s)	Solubility coefficient (S) (cm^3 (STP)/cm^3·MPa)
Polyethylene + Methane	40	7	1.6	0.57
Polyethylene + Carbon dioxide	40	4	4	1.4
Polyamide 11 + Methane	70	10	0.62	0.44
Polyamide 11 + Carbon dioxide	70	4	1.0	2.3

4. SIMULATION OF MASS DIFFUSION OF DIFFERENT GASES IN PE AND PA11

The above discussion only serves as a general background for the simulation. The experimental data is required for the accurate simulation. The required experimental information are obtained from literature [2] and are shown in Table 1. Modeling and simulation were carried out in Abaqus software as it has built-in mass diffusion analysis. Two case studies were performed below to check suitability of proposed method.

4.1 CASE STUDY 1

A simple 2D section of 2 cm cross section has been modelled in Abaqus software and the following values are applied from the table 1. The values are given for Polyethylene material

- Coefficient of diffusivity – 1.6 (methane), 4 (carbon dioxide)
- Concentration for material – 1
- Solubility of material – 0.57 (methane), 1.4 (carbon dioxide)
- Steady state
- Concentration on the inner edge – 0.8
- Concentration on the outer edge – 0

The geometry, mesh and boundary conditions are shown in Figure 10-12. The concentration distribution is also shown in Figure 13-14.

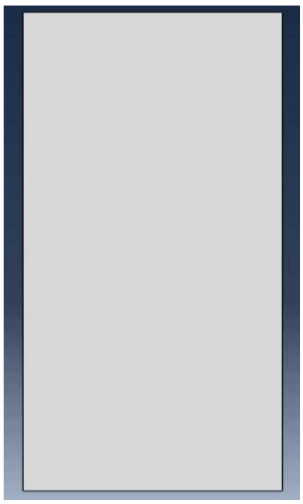

- Figure 10: Geometry

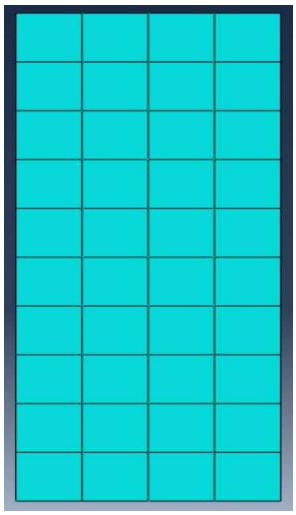

- Figure 11: Mesh

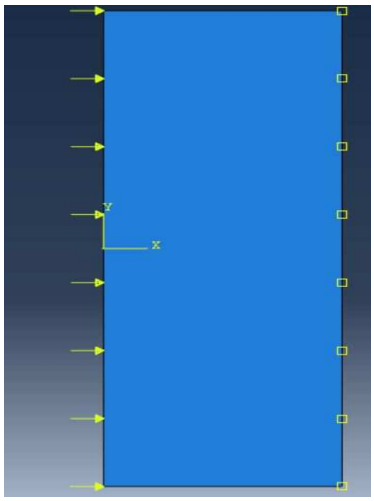

- Figure 12: BC's and Load

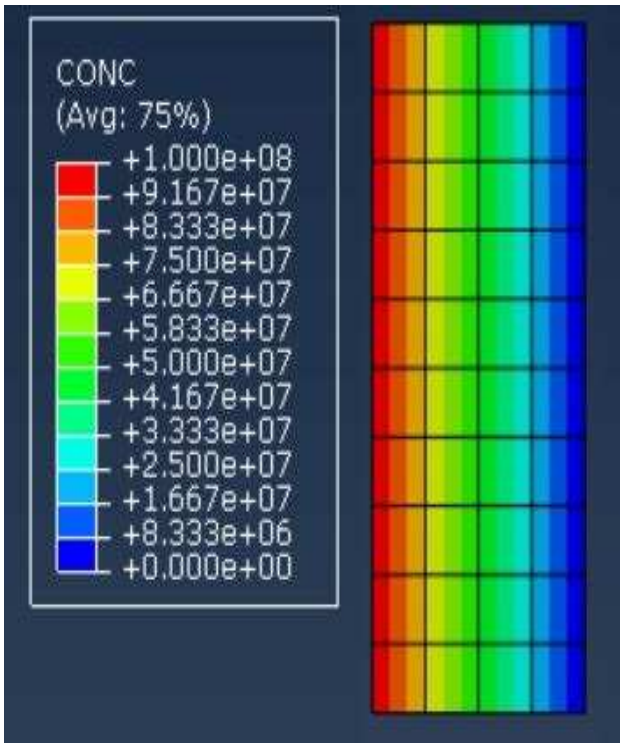

Figure 13: Concentration distribution of methane in PE

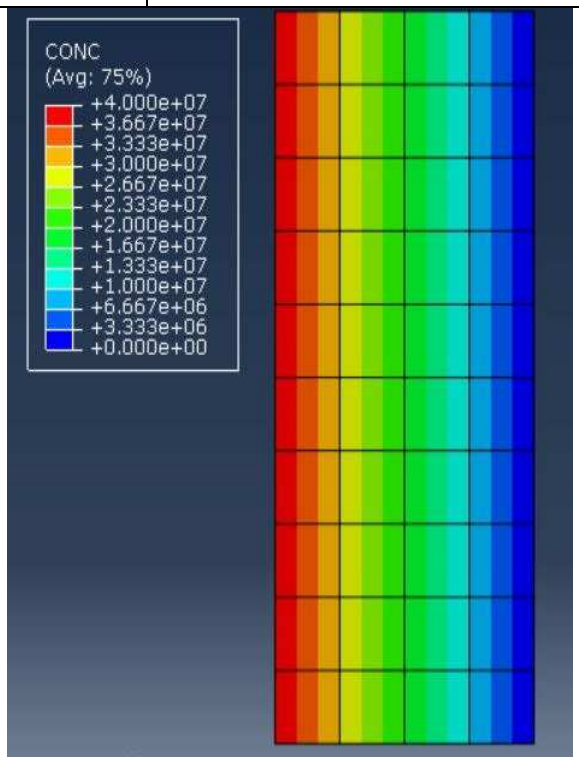

Figure 14: Concentration distribution of carbon dioxide in PE

A simple 2D section of 2 cm cross section has been modelled in Abaqus software and the following values are applied from the table 1. The values are given for Polyamide 11 material

- Coefficient of diffusivity – 0.62 (methane), 1 (carbon dioxide)
- Concentration for material – 1
- Solubility of material – 0.44 (methane), 2.3 (carbon dioxide)
- Steady state
- Concentration on the inner edge – 0.8
- Concentration on the outer edge – 0

The geometry, mesh and boundary conditions are shown in Figure 15-17. The concentration distribution is also shown in Figure 18-19.

- Figure 15: Geometry

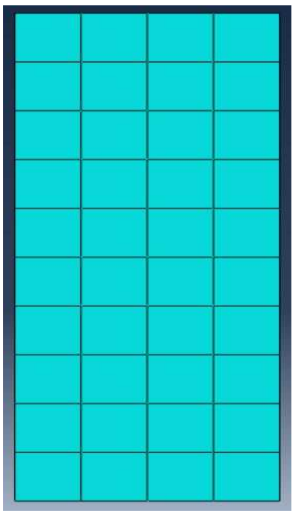

- Figure 16: Mesh

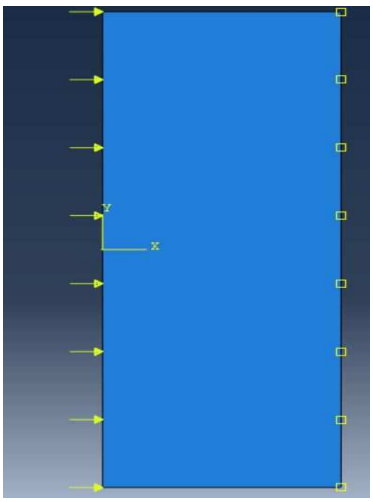

- Figure 17: BC's and Load

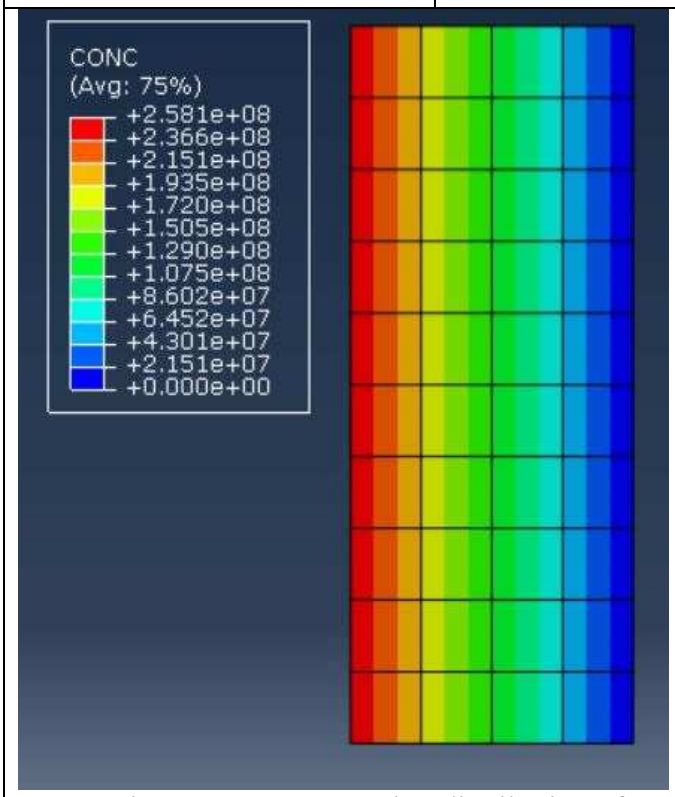

Figure 18: Concentration distribution of methane in PA 11

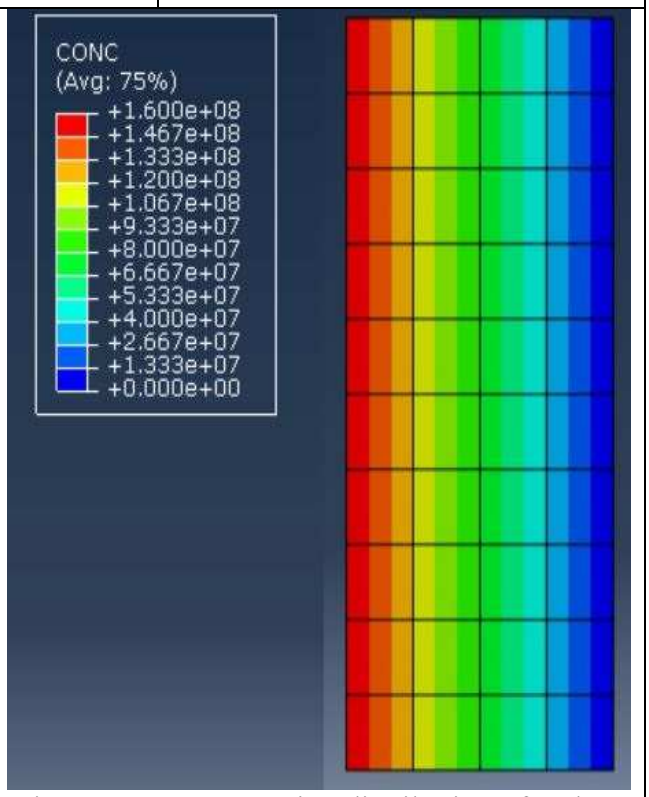

Figure 19: Concentration distribution of carbon dioxide in PA 11

Description of any Problems/Challenges

The project progress is satisfactory according to the schedule of tasks table. Good communications between the PIs, students and program director is well maintained. There are a few technical challenges identified and will be addressed in the future quarters, which is listed as follow:

Computer power for simulation:
The simulation requires massive amount of calculations, which also reuqires a high performance computer to compute the data. CU has been working on purchasing a new server to perform all the simulations for the project, which will improve the simulation time compares now.

PA samples acquistion from industrial parterner:
PA materials samples have been received from the industrial patterned. Testing plans are current been discussed between CU Denver and ASU and will be reported in the future reports.

(c) Planned Activities for the Next Quarter

Besides the planned activities mentioned in section (b), here are the future work for the next quarter:

Development of 3D EFG simulation model:
Both simulations model built in this quarter gave us promising results. In next quarter, we will develop the element-free Galerkin's method (EFG) to verify the results and also develop the 3D model. The current EFG codes are two-dimensional and unrealistic for the actually pipe geometry. A new CAAP PhD student has been assigned to work on the modeling part at CU, which is significantly different from the proposed modeling work for another DOT CAAP13 project. Due to the complexity of the problem, both self-developed codes and commercial software packages with careful customization will be evaluated first. The first version of the 3D EFG simulation codes is expected to be running and be valided in Q2.

Imaging system optimization: Within Q1, the CAAP team at CU further improved the imaging system resolution with the collateral support from CAAP 13. The phase information of the measured NFMW signals has been successfully extracted, however further post-processing and data fusion techniques are needed to better understand the acquired images, which are under investigation. More results are expected to be generated and reported at the end of Q2.

XFEM simulation with multiphsics damage coupling: Following the previous kick offmeeting and phoen discussions, it was identified that other environmental damage may contribute to the final failure of pipeline systems, such as diffusion. ASU team is working on a general methodology to include this type of damage in the current simulation framework,

REFERENCES

1. Chaoui, K., et al., *Failure Analysis of Polyethylene Gas Pipes*, in *Safety, Reliability and Risks Associated with Water, Oil and Gas Pipelines*, G. Pluvinage and M. Elwany, Editors. 2008, Springer Netherlands. p. 131-163.
2. Argon, A.S., *The physics of deformation and fracture of polymers*. 2013: Cambridge University Press.
3. Kwon, H.J. and P.Y.B. Jar, *Toughness of high-density polyethylene in plane-strain fracture.* Polymer Engineering & Science, 2006. **46**(10): p. 1428-1432.
4. Anderson, T.L., *Fracture mechanics: fundamentals and applications*. 2005: CRC press.
5. Ba and M.T. Kazemi, *Determination of fracture energy, process zone longth and brittleness number from size effect, with application to rock and conerete.* International Journal of Fracture, 1990. **44**(2): p. 111-131.